

## Using Thermal Treatment Process to Enhance Anodic Oxidation TiO<sub>2</sub> Nanotubes with High Degradation Effect of Methylene Blue

Wei Chien,<sup>1</sup> Chi-Yu Lin,<sup>2</sup> Shang-Te Tsai,<sup>3</sup>  
Cheng-Fu Yang,<sup>4\*</sup> Shih-Tung Shu,<sup>5</sup> and Chiu-Chen Chang<sup>5</sup>

<sup>1</sup>Department of School of Electronic and Information Engineering, Qinzhou University,  
No. 89, Xihuan Nanlu, Qinzhou 535000, Qinzhou, Guangxi, China

<sup>2</sup>Department of Aero-Electronic Engineering, Air Force Institute of Technology,  
No. 198, Jieshou W. Rd., Gangshan Townwhip, Kaohsiung County 820, Kaohsiung, Taiwan

<sup>3</sup>Department of Economics and Management, Ningde Normal University,  
No. 1, Xuanyuan Road, Dongqiao Economic Development Zone Ningde City 352100, China

<sup>4</sup>Department of Chemical and Materials Engineering, National University of Kaohsiung, Kaohsiung,  
700, Kaohsiung University Road, Nanzih District, Kaohsiung 811, Taiwan

<sup>5</sup>College of Management, National Kaohsiung First University of Science and Technology  
No. 2, Jhuoyue Road., Nanzih Dist., Kaohsiung City 811, Taiwan

(Received October 29, 2017; accepted January 10, 2018)

**Keywords:** TiO<sub>2</sub> nanotube (TNT) arrays, anatase phase, moss decomposition, methylene blue

In this study, TiO<sub>2</sub> nanotube (TNT) arrays were grown on Ti metal using the anodic oxidation method. After finding the parameters to grow TNT arrays with maximum specific surface area, the TNT arrays were annealed over a temperature range of 350–600 °C. From the X-ray diffraction (XRD) patterns we found that the as-deposited TNT arrays revealed an amorphous phase. As the annealing temperature was increased from 350 to 500 °C, the diffraction intensity of the anatase phase increased. As the annealing temperature reached 600 °C, both the anatase phase and the rutile phase were observed in the arrays. The TNT arrays with different annealing temperatures were used to carry out experiments in moss decomposition and methylene blue degradation. The surface observation was used to judge the effect on moss decomposition, and the Beer–Lambert law was used to judge the effect on methylene blue degradation. We show that TNT arrays annealed at 500 °C functioned best in both moss decomposition and methylene blue degradation because of the presence of only the anatase phase.

### 1. Introduction

Methylene blue, also known as methylthioninium chloride, is a medication and dye. With the progression of global industrialization, environmental pollution has become a more serious issue and thus has received considerable attention. Dye compounds being released from textile factories as effluent are a significant source of pollution and eutrophication in aquatic ecosystems and environments. Techniques for the removal of dyes have been intensively

---

\*Corresponding author: e-mail: cfyang@nuk.edu.tw  
<http://dx.doi.org/10.18494/SAM.2018.1820>

studied recently because international environmental standards are becoming more stringent and significant. In the past, many methods had been investigated to lower diminish the concentration of methylene blue in water. Three-dimensional structures of copper sulfide (CuS) are favored for methylene blue degradation because they are nontoxic, inexpensive, and stable under ambient conditions.<sup>(1)</sup> They have efficient catalytic ability because of their high surface area to volume ratio allowing for better contact between the reactants and CuS. Maehara *et al.* used radio frequency (RF) plasma in water to degrade methylene blue and found that the fraction of decomposition of methylene blue and the intensity of the spectral line from OH radicals increased with RF power.<sup>(2)</sup> Vanaja *et al.* successfully synthesized silver nanoparticles using *Morinda tinctoria* leaf extract under different pH values, and they used synthesized silver nanoparticles to degrade methylene blue under irradiation with sunlight.<sup>(3)</sup>

TiO<sub>2</sub>-based materials are used in a wide range of applications because of their excellent properties such as nontoxicity, high catalytic activity, low cost, and long-term stability. For these reasons, TiO<sub>2</sub>-based materials are generally considered to be the best photocatalysts with the ability to detoxify water from a number of organic pollutants. However, the relatively wide band gap and intense recombination of electron–hole pairs in TiO<sub>2</sub>-based materials limit their efficiency in photo-electrochemical applications. Materials of nanoscale size with a high surface area and a high fraction of surface atoms have been studied because of their unique optical, electronic, and catalytic properties. TiO<sub>2</sub>-based materials are biologically stable and cheap, which makes them a very common semiconductor used for dye degradation. TiO<sub>2</sub>-based materials of nanoscale size are good photocatalysts for the degradation of organic and inorganic pollutants in the air and water and have broad prospects for applications.<sup>(4)</sup> Due to their large band gap, some alterations can be made to improve their photocatalytic abilities, such as the synthesis of 6,13-pentacenequinone/TiO<sub>2</sub>. TiO<sub>2</sub>-based materials in conjunction with ultraviolet light can also be utilized for the decolorization and detoxification of diluted colored water waste containing such compounds as alizarin, azo dyes, methyl red, and methylene blue.<sup>(5)</sup> Reduced graphene TiO<sub>2</sub>-based materials can also act as photocatalysts for the degradation of methyl orange (MO), azo-dyes, and pharmaceutical water waste.<sup>(6)</sup> Zuo *et al.* prepared TiO<sub>2</sub>/diatomite composite as a photocatalyst, which was formed by loading TiO<sub>2</sub> on the surface of diatomite, and which worked by absorbing organic compounds with diatomite and degrading them with TiO<sub>2</sub>-based composites.<sup>(7)</sup>

All these methods have problems of complicated processes for the preparation the TiO<sub>2</sub>-based photocatalytic materials. Anodic TiO<sub>2</sub> nanotube (TNT) arrays have attracted growing interest because of their unique morphology and physicochemical properties.<sup>(8)</sup> In the past, we have used the TNT arrays to fabricate dye-sensitized solar cells (DSSCs).<sup>(8)</sup> The TNT can also be used as the sensor materials. For example, Kwon *et al.* prepared TNT arrays for use as C<sub>2</sub>H<sub>5</sub>OH gas sensors by anodizing Ti thin foils.<sup>(9)</sup> We have shown that the measured photovoltaic performance of the DSSCs was dependent on the length of the TNT arrays. In the past, there have been many studies using the nanostructured TiO<sub>2</sub>-based materials as photocatalysts to degrade industrial dyes.<sup>(10)</sup> For example, Yu *et al.* used TiO<sub>2</sub> (anatase) films and nano-sized TiO<sub>2</sub> particles as photocatalysts and studied their effects on the decomposition of the pollutant dye MO.<sup>(11)</sup> Few researchers used the TNT arrays as photocatalysts to degrade

pollutant dyes. In this paper we discuss the novel effect of crystalline phases on methylene blue degradation. We found that when the TNT arrays were amorphous, they had almost no photocatalytic effect because they could not decompose methylene blue. Our second important observation is that, if we annealed the TNT arrays in air, we could change the amorphous phase to the anatase phase and the photocatalytic effect could thereby be really observed and improved. The photocatalytic activity of the synthesized TNT arrays was examined by the experiments in moss decomposition and methylene blue degradation under UV-light irradiation. We have shown that, even if the concentration of methylene blue was only 5 ppm, the synthesized TNT arrays could effectively degrade the dye over 50% with 100 min of exposure.

## 2. Experimental Methods

In this research, we fabricated ordered TNT arrays on anodizing titanium (Ti) foil (Aldrich, 99.7% purity) as square discs ( $20 \times 20 \text{ mm}^2$ ) at a constant voltage of 50 V. Ti foils, 0.25 mm thick, were degreased by ultrasonication in acetone and then isopropanol for about 30 min, followed by rinsing with deionized (DI) water, and finally dried in air before being used. The electrolyte solutions contained ammonium fluoride ( $\text{NH}_4\text{F}$ , 99.9%) in ethylene glycol in the presence of  $\text{H}_2\text{O}$  (2 vol%,  $\text{pH} = 6.8$ ) with anodization for varied parameters. Highly ordered TNT arrays over large areas were prepared by potentiostatic anodization in a two-electrode electrochemical cell with a platinum (Pt) sheet as the counter electrode. All anodization experiments were carried out at room temperature. After being grown, the TNT arrays were rinsed with ethanol, dried in air, and annealed at  $150 \text{ }^\circ\text{C}$  for 2 h to remove organic solvents. The detailed processes for preparing the TNT arrays are shown in Ref. 8. In this study, the optimum parameters to grow the TNT arrays were 0.6 wt%  $\text{NH}_4\text{F}$ , 2 vol%  $\text{H}_2\text{O}$ , ethylene glycol 100 ml, and anodization time 2 h. The TNT arrays had a length of  $10.0 \text{ }\mu\text{m}$  and an inner diameter of 111 nm, as shown in Figs. 1(a) and 1(b), respectively. It is evident that highly ordered TNT arrays consisting of very regular tubes with uniform inner diameters have been obtained.

The grown TNT arrays were then crystallized at different temperatures ( $350\text{--}600 \text{ }^\circ\text{C}$ ) for 1 h in air. If the annealing temperature was higher than  $600 \text{ }^\circ\text{C}$ , the TNT arrays would burst into

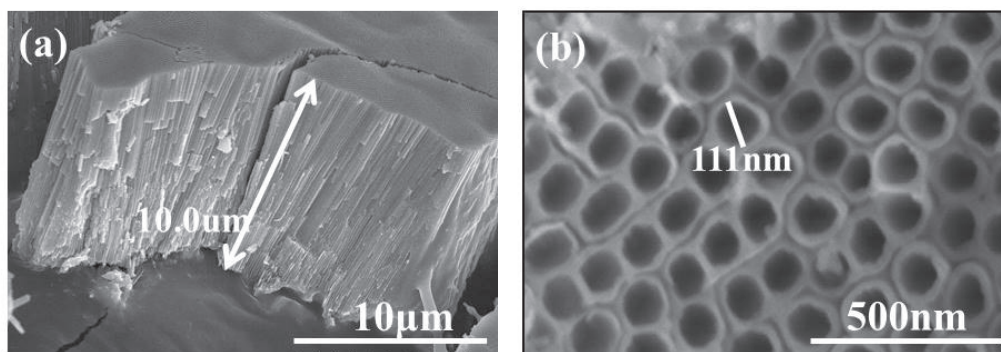


Fig. 1. TNT arrays grown and used in this study. (a) Side view and (b) top view.

pieces and could not be used as photocatalytic materials to decompose the moss and degrade the pollutant dyes. X-ray diffraction (XRD) patterns were used to characterize the crystalline structure of the anodized TNT arrays prepared at different annealing temperatures. The XRD analysis of the TNT arrays was done using a Bruker diffractometer, Cu-K X-rays of wavelength ( $\lambda$ ) = 1.5406 Å, and data was taken for the  $2\theta$  range from 20 to 80°. The TNT arrays prepared at different annealing temperatures were used to carry out experiments on moss decomposition and methylene blue degradation. For the experiment on moss decomposition, wetted moss (0.5 g) was coated on the surfaces of the grown and annealed TNT arrays. For the experiment on methylene blue degradation, 0.5 ppm solution of methylene blue was prepared and the  $10 \times 10 \text{ mm}^2$  TNT arrays were dipped in 5 ml of this solution. After that, those samples were exposed to ultraviolet light at a wavelength of 265 nm for different lengths of time. For the experiment on moss decomposition, as Fig. 2(a) shows, the duration of exposure was changed from 0 to 72 h. For the experiment on methylene blue degradation, as Fig. 2(b) shows, the duration was changed from 0 to 100 min. Observation of the surface was used to judge the effect on moss decomposition and the Beer–Lambert law was used to judge the effect on methylene blue degradation. For measuring the variations in concentration of the methylene blue liquid, the values of five samples were used to determine an average value. The optical transmittance spectra of the methylene blue solutions were measured using a Hitachi U-3300 UV-Vis spectrophotometer in the 200 to 700 nm wavelength range.

### 3. Results and Discussion

To achieve high degradation effects on organic and inorganic pollutants, the preparation of TNT arrays forming the crystalline phases is very important, because crystallization of TNT arrays influences their photocatalytic effects. Figure 3 shows the XRD patterns of our TNT arrays as a function of annealing temperature. For the as-grown TNT arrays, only the Ti phase could be observed and no anatase phase and or rutile phase were revealed. When the TNT arrays were annealed at 350 °C, strong peaks occurred around 25.5° for the (101) diffraction peak of the anatase phase. As Fig. 3 shows, when the annealing temperature of the TNT arrays was increased from 350 to 500 °C, the diffraction intensity of the (101) peak increased. The  $2\theta$  value of the (101) diffraction peak was almost unchanged and the full width at half maximum

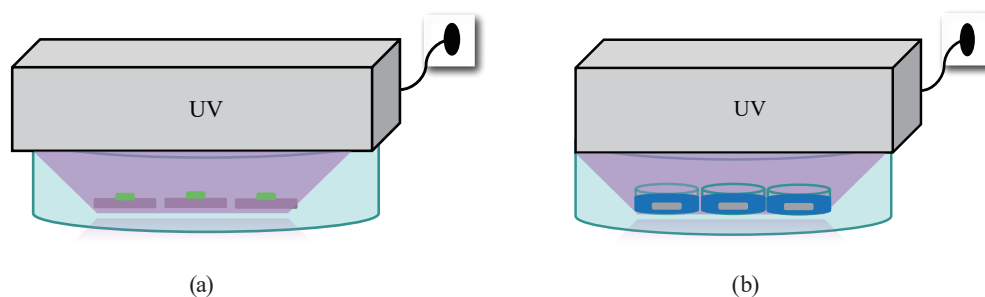


Fig. 2. (Color online) Set-ups for the experiments on (a) moss decomposition and (b) methylene blue degradation.

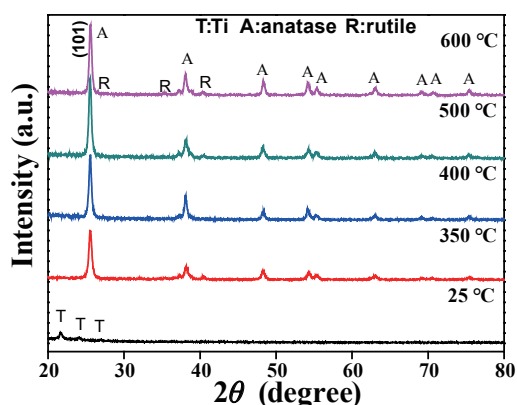


Fig. 3. (Color online) XRD patterns of TNT arrays as a function of annealing temperature.

(FWHM) values for the (101) diffraction peak decreased from  $2\theta = 0.48$  to  $2\theta = 0.44$ . These results suggest that the TNT arrays annealed at 350–500 °C would have a stable anatase phase regardless of the annealing temperature. When the annealing temperature was 600 °C, the  $2\theta$  value of the (101) diffraction peak was unchanged, the diffraction intensity of the (101) peak decreased, the FWHM value for the (101) diffraction peak increased to  $2\theta = 0.46$ , and the diffraction peaks for the rutile phase were readily observed. Because the different annealing temperatures of TNT arrays produced different results with respect to crystallinity, we believe that they will have different effects on moss decomposition and methylene blue degradation.

Figure 4 shows the surfaces in the experiment on moss decomposition as a function of the annealing temperature of the TNT arrays and irradiation time with UV light. As Fig. 4 shows, the moss on the unannealed (25 °C) TNT arrays was almost unchanged, even when the time of irradiation with UV light was 72 h. These results indicate that the TNT arrays with an amorphous phase have almost no photocatalytic effect. As the annealed TNT arrays were used to carry out the experiment, the moss decreased as the irradiation time with UV light increased and the TNT arrays annealed at 500 °C had the greatest effect on moss decomposition. Comparing the results in Fig. 4 with the crystalline phase shown in Fig. 3, we believe the TNT arrays with a higher diffraction intensity of the anatase phase have a higher photocatalytic effect and hence produce this result.

The transmittance spectra of methylene blue solutions resulting from using TNT arrays annealed at 350 and 500 °C as the photocatalytic materials are shown in Fig. 5. The intensities of three strong absorption bands of methylene blue located at 246, 293, and 664 nm decreased gradually with increasing irradiation time with UV light. When 350 °C-annealed TNT arrays were the photocatalytic materials, the average intensity of the strong absorption band at 664 nm decreased from 91.3 to 83.07, 75.3, 68.3, and 60.4% as the irradiation time increased from 20 to 40, 60, 80, and 100 min [Fig. 5 (a)]. When 500 °C-annealed TNT arrays were the photocatalytic materials, the average intensity of the strong absorption band located at 664 nm decreased from 88.2 to 78.8, 67.7, 57.5, and 48.2% as the UV-light irradiation time increased from 20 min to 40 min, 60 min, 80 min, and 100 min [Fig. 5 (b)]. These results demonstrate that the transmittance spectra of methylene blue solutions can be used to judge the effect on methylene

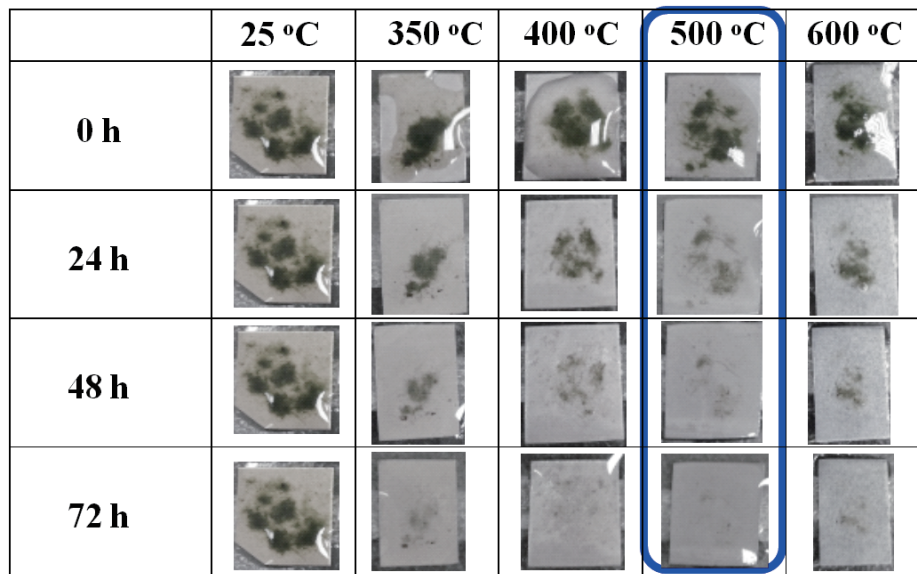


Fig. 4. (Color online) Surfaces of the TNT arrays in experiment on moss decomposition as a function of annealing temperature and time of irradiation with UV light.

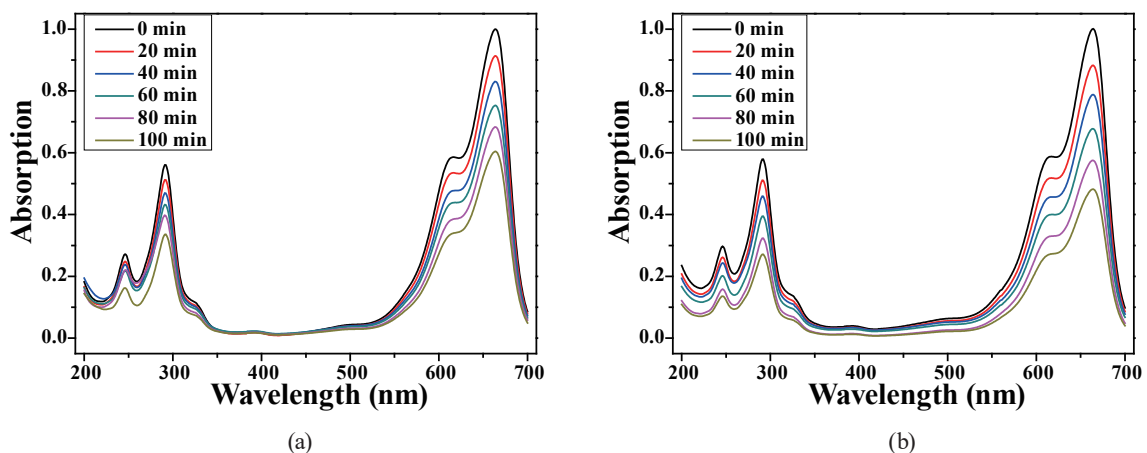


Fig. 5. (Color online) Ultraviolet-visible spectra of the methylene blue solution as a function of the annealing temperature of TNT arrays and irradiation time with UV light: annealed at (a) 350 °C and (b) 500 °C.

blue degradation. The results in Fig. 5 also indicate that different annealing temperatures cause the TNT arrays to have different crystalline structures and consequently produce different results in methylene blue degradation.

The Beer–Lambert law (or Beer’s law) is the linear relationship between absorbance and concentration of an absorbing species. The Beer-Lambert law relates the attenuation of light to the properties of the material through which the light is traveling. The law is commonly applied to analytical measurements in chemistry and is used to understand attenuation in physical optics for photons, neutrons, or rarefied gases.

$$A = \log(I_o/I) = abc \quad (1)$$

Here,  $A$  is the absorbance,  $I_o$  is the incident light,  $I$  is the transmitted light,  $a$  is the molar absorptivity with units of  $\text{L mol}^{-1} \text{cm}^{-1}$ ,  $b$  is the path length (here is the width of the quartz cell containing the methylene blue solution), and  $c$  the concentration of the compound in solution, expressed in  $\text{mol L}^{-1}$ .<sup>(2)</sup> The relationship between absorbance (by measuring the intensity of the peak at 664 nm) and the irradiation time of methylene blue degradation experiment using the TNT arrays annealed at different temperatures is shown in Fig. 6. As compared with the unannealed TNT arrays, annealed TNT arrays exhibit improved photocatalytic response with respect to the degradation of methylene blue under UV-light irradiation. With exposure, the absorbance of the spectral peak (664 nm) decreased monotonically as the irradiation time with UV light increased. Using 500 °C-annealed TNT arrays as the photocatalyst resulted in a line with a larger slope than those using TNT arrays annealed at other temperatures. This means that the 500 °C-annealed TNT arrays have the optimum photocatalytic effect in methylene blue degradation. These results match the variation in the crystalline phase of TNT arrays shown in Fig. 3 and the experiment of moss decomposition shown in Fig. 4.

Langmuir–Hinshelwood (LH) kinetics is the most commonly used kinetic expression to explain the kinetics of the heterogeneous catalytic processes. The LH rate expression has been successfully used for heterogeneous photocatalytic degradation to determine the relationship between the initial degradation rate and the initial concentration of the organic substrate.<sup>(12)</sup>

$$R = -dC/dt = kC \quad (2)$$

$$\int_{C_o}^C dC/C = \int_0^t kt \quad (3)$$

$$\ln(C/C_o) = -kt \quad (4)$$

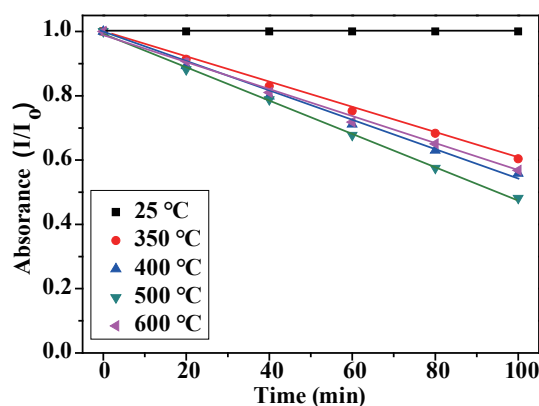


Fig. 6. (Color online) Absorption of methylene blue solutions as a function of annealing temperature of TNT arrays and irradiation time with UV light.

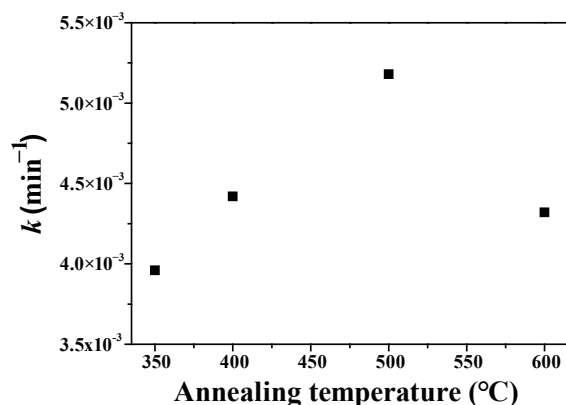


Fig. 7. Rate constants for the degradation of the methylene blue as a function of the annealing temperature of TNT arrays and irradiation time with UV light.

Here,  $R$  is the reaction rate,  $C$  and  $C_0$  are the concentrations of methylene blue after and before irradiation with UV light, respectively,  $t$  is the reaction time, and  $k$  is the reaction constant. Figure 7 shows that as for the reaction constant first increased with increasing annealing temperature, reached a maximum 500 °C-annealed TNT array, and then decreased as the annealing temperature was further increased. When the 500 °C-annealed TNT arrays are used as the photocatalyst, even if the concentration of methylene blue solution is only 5 ppm, a  $k$  value of  $5.18 \times 10^{-3} \text{ min}^{-1}$  is really obtained. These results suggest we can use TNT arrays as the photocatalysts under solar radiation. These results also indicate that we can use annealed TNT arrays as photocatalysts to decompose unwanted or harmful organisms (moss) as well as environmentally polluting dyes and that they have the ability to detoxify water contaminated with a number of organic pollutants.

#### 4. Conclusion

In this study, the photocatalytic effect of TNT arrays annealed at different temperatures from 300–600 °C were successfully demonstrated in experiments on moss decomposition and methylene blue degradation. As the annealing temperature of the TNT arrays was increased from 350 to 500 °C, only the anatase phase was observed; when 600 °C was used as the annealing temperature, the rutile phase was also observed. In experiments on moss decomposition and methylene blue degradation we found the 500 °C-annealed TNT arrays demonstrated the maximum photocatalyst effect. Even when the concentration of the methylene blue solution was only 5 ppm, the concentration could be decreased 48.2% after illumination with 254 nm UV-light for 100 min.



## References

- 1 Q. W. Shu, J. Lan, M. X. Gao, J. Wang, and C. Z. Huang: *Cryst. Eng. Commun.* **17** (2015) 1374.
- 2 T. Maehara, I. Miyamoto, K. Kurokawa, Y. Hashimoto, A. Iwamae, M. Kuramoto, H. Yamashita, S. Mukasa, H. Toyota, S. Nomura, and A. Kawashima: *Plasma Chem. Plasma Process.* **28** (2008) 467.
- 3 M. Vanaja, K. Paulkumar, M. Baburaja, S. Rajeshkumar, G. Gnanajobitha, C. Malarkodi, M. Sivakavinesan, and G. Annadurai: *Bioinorg. Chem. Appl.* **2014** (2014) Article ID 742346.
- 4 W. Mekprasart and W. Pecharapa: *Proc. Eco-Energy and Materials Science and Engineering Symp.* **9** (2011) 509.
- 5 H. Lachheba, E. Puzenata, A. Houasb, M. Ksibib, E. Elalouib, C. Guillarda, and J. Herrmanna: *Appl. Catal., B* **39** (2002) 75.
- 6 L. M. Pastrana-Martínez, S. Morales-Torres, V. Likodimos, J. L. Figueiredo, J. L. Faria, and P. Falaras: *Appl. Catal., A* **19** (2012) 3676.
- 7 R. F. Zuo, G. X. Du, W. W. Zhang, L. H. Liu, Y. M. Liu, L. F. Mei, and Z. H. Li: *Adv. Mater. Sci. Eng.* **2014** (2014) Article ID 170148
- 8 C. G. Kuo, C. F. Yang, L. R. Hwang, and J. S. Huang: *Int. J. Photoenergy* **2013** (2013) Article ID 650973.
- 9 Y. J. Kwon, H. Kim, S. M. Lee, I. J. Chin, T. Y. Seong, W. I. Lee, and C. M. Lee: *Sens. Actuators, B* **173** (2012) 441.
- 10 S. H. Kang, T. H. Fang, T. H. Chen, Y. J. Hsiao, Z. H. Hong, C. H. Chuang, and L. Riccobono: *Microsyst. Technol.* **10** (2014) 515.
- 11 L. H. Yu, J. Y. Xi, M. D. Li, H. T. Chan, T. Su, D. L. Phillips, and W. K. Chan: *Phys. Chem. Chem. Phys.* **14** (2012) 3589.
- 12 S. Khezrianjoo and H. D. Revanasiddappa: *Chem. Sci. J.* **2012** (2012) CSJ-85.